Basin Effects in Seismic Design: Efficiency of Numerical Tools in Reproducing Complex Seismic Wavefields

K. Makra
Earthquake Planning and Protection Organization – ITSAK, Thessaloniki, Greece

F. Gelagoti
National Technical University of Athens, Greece

O.-J. Ktenidou
Université Joseph Fourier - CNRS, Institute of Earth Sciences (ISTERRE), Grenoble, France

K. Pitilakis
Aristotle University of Thessaloniki, Greece

SUMMARY:
We present seismic response results of 3 different numerical tools (FDDVS, FLAC and ABAQUS) and check their efficiency in reproducing complex seismic wavefields up to 10Hz in an ”idealised“ two-dimensional basin for a number of cases, varying the parameters that most affect propagation of seismic waves. In a second step, making use of the advantage that both equivalent linear and nonlinear soil behaviour models are available in FLAC and ABAQUS respectively, we check the coupling of non-linear effects with the geometrical characteristics of the basin for a series of input motion levels (0.1g, 0.3g, 0.5g and 1g outcrop motion). The agreement in the results of the 3 numerical tools is surprisingly good. This could subsequently consolidate their use in order to form practical guidelines that introduce basin effects in the seismic design of structures

Keywords: Basin Effects, Building Codes, Aggravation Factor, Non-linear Behaviour

1. INTRODUCTION

It is widely recognized that local geological conditions have a large impact on ground motion at a given site. The geometry of the subsoil structure, the variation of soil types and its properties with depth, the lateral discontinuities, and the surface topography are at the origin of large amplification of ground motion and have been correlated to damage distribution during destructive earthquakes (Aki, 1993; Bard, 1994; Faccioli, 1991; 1996; Chávez-García et al., 1996; Kawase, 1996). The effects of subsurface geometry on seismic ground motion have been well recognized during the past decades. Euroseistest is a striking example (Pitilakis et al., 2011). Euroseistest is established in a shallow valley. The shape of this valley has been shown to control the characteristics of ground motion (Raptakis et al, 2000; Chávez-García et al., 2000; Makra et al., 2005). Makra et al. (2001) and Makra & Raptakis (2007) quantified, only for this valley, the additional amplification introduced by consideration of the lateral heterogeneity, making use of aggravation factors relatively to 1D response.

The complexity of the effects of subsurface geometry on seismic ground motion made it impossible until now to include systematically such effects in earthquake hazard assessment and risk mitigation. This is shown by the fact that the majority of modern seismic codes do not include any provision for basin and topography effects. In the framework of European research project NERA, one research activity is dedicated to making solid, simple and practical recommendations to incorporate the aforementioned effects into seismic design (microzonation studies, building codes, critical facilities, etc.). Such recommendations will be based on extensive numerical simulations on basin models with varying mechanical and geometrical characteristics as well as different incoming wavefields. Special attention is paid to non-linear effects coupled with those of the geometrical characteristics.

In this context, we present the capabilities of 3 different numerical tools (FDDVS, FLAC and ABAQUS) and check their efficiency in reproducing complex seismic wavefields up to 10Hz in an ”idealised“ two-dimensional basin for a number of cases, varying the parameters that most affect propagation of seismic waves (e.g. damping, Vs contrast) in the linear range. Taking advantage that both equivalent linear and nonlinear soil behavior models are available in FLAC and ABAQUS software packages respectively, we check the coupling of non-linear effects with the geometrical characteristics of the basin for a series of input motion levels, corresponding to outcrop motion of 0.1g, 0.3g, 0.5g and 1g. Extensive comparisons are made both in time (synthetic velocity time histories) and frequency (amplification transfer functions) domain, as well as in terms of aggravation factors at specific locations along the surface of valley. The aggravation factor is defined as the ratio between 2D and 1D response spectra. It aims to quantify the additional amplification caused due to the effect of the surface waves, which are locally generated at the lateral discontinuities (basin edges).

2. 2D VALLEY MODEL AND NUMERICAL METHODS USED

2.1. Geometry, dynamic properties and excitation wavefield

The 2D valley configuration is a flat symmetrical trapezoidal valley consisting of two layers (matB-soil and matA-rock). The total extent of the model is 3200m. The length of the basin is 1200m (surface trace) bounded with 1km (from each side) of mat A. The max depth of the basin is 100m and the inclination angle of the lateral boundary of the valley, a, is 45°. Figure 1 shows only half of the valley model taking advantage of the symmetry conditions. This model is tested for a number of cases, varying the parameters that most affect propagation of seismic waves in the linear and nonlinear range. The dynamic properties of materials, type of excitation and amplitude of corresponding outcrop motion, as well as the analysis type for each case are given in table 1. For the equivalent linear and nonlinear analysis, the shear modulus and damping variation with increasing shear strain is described in figure 2 (left). Figure 2 (right) shows the acceleration source-time-function of input motion and its fourier amplitude spectra corresponding to 0.1g at the surface used as incoming wavefield at 300 m

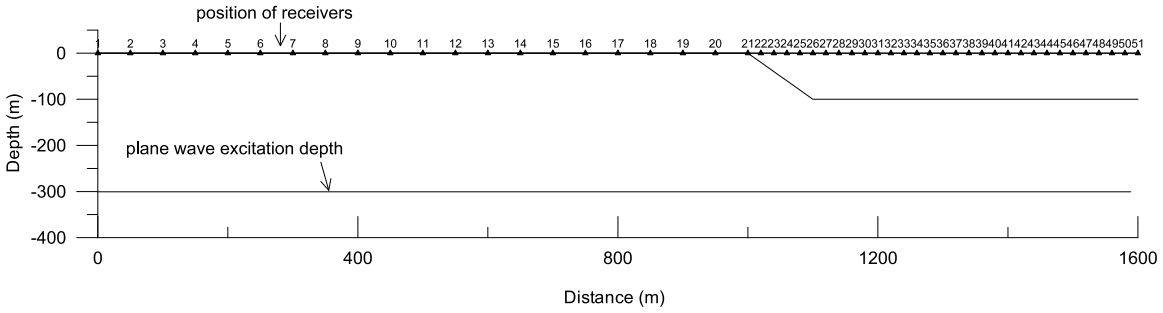

Figure 1. 2D Valley configuration (symmetric part)

Table 1. Summary of dynamic properties of materials, type of excitation and amplitude of corresponding outcrop motion, and analysis type for each case

		Case 1	Case 2	Case 4	Case 6	Case 7	Case 8	Case 9
Mat A	Vs (m/sec) / Qs[1]	2500 / ∞	2500 / 100					
	Vp (m/sec) / Qp	4500 / ∞	4500 / 200					
	ρ (kg/m^3)	2500						
Mat B	Vs (m/sec) / Qs	625 / ∞	625 / 50	417 / 50				
	Vp (m/sec) / Qp	2500 / ∞	2500 / 100	2000 / 100				
	ρ (kg/m^3)	2200						
	Excitation	SV vertical incident						
	outcrop rock amplitude	0.1g	0.1g	0.1g	0.1g	0.3g	0.5g	1.0g
	Analyses type	Elastic	Visco-elastic	Visco-elastic	Equiv. Linear Non Linear	Non Linear	Non Linear	Non Linear

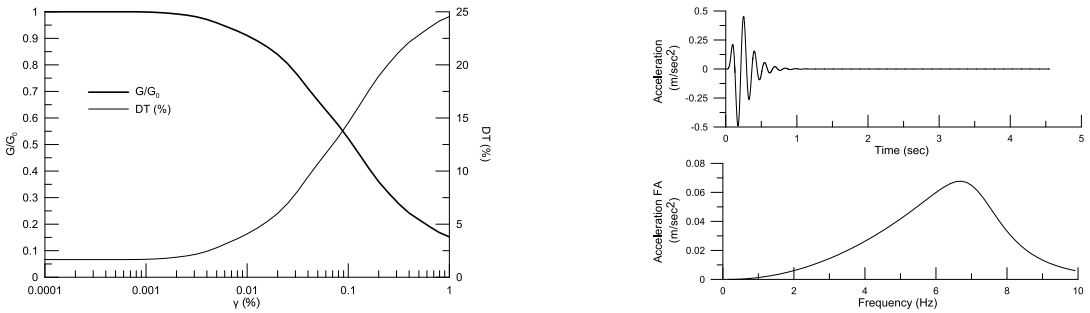

Figure 2. G/G_0-γ-DT(%) curve used to describe the non-linear behavior of soil material B (left). Incoming wavefield acceleration time history and Fourier spectra (right)

depth. For cases 7-9 (table 1), incoming acceleration wavefield is scaled by a constant factor of 3, 5 and 10 times, respectively, to obtain input motion for higher input acceleration levels.

2.2. Software

Three different numerical tools (FDDVS, ABAQUS and FLAC2D) are used to model propagation of seismic waves for the above 2D valley configuration in order to check their efficiency in reproducing seismic wavefields up to 10Hz. A short description of the main features of these tools is given below.

2.2.1. 2DFDVS

2DFDVS computational tool is based on a finite-difference scheme to simulate seismic wave propagation in heterogeneous viscoelastic structures. The computational algorithm is based on the explicit heterogeneous finite-difference scheme solving equations of motion in the heterogeneous viscoelastic medium with material discontinuities. The computational region is an area with the top boundary representing a planar free surface, and the bottom and lateral boundaries representing non-reflecting boundaries. A uniform rectangular spatial grid is used to cover the computational region. The size of the spatial grid as well as the time sampling are properly chosen to serve stability and accuracy of the results for frequencies up to 10Hz. Namely, for the cases described in table 1, the grid size is 5m for both horizontal and vertical directions. The analysis time step is assigned to 0.0005sec according to grid size and maximum P-wave velocity in the model. The rheology of the medium corresponds to the generalized Maxwell body. This makes possible to account both for spatially varying quality factors of P and S waves and for constant Q values for the frequency range of interest. Details on this algorithm could be found in Moczo et al. 2007, Moczo et al. 2004, Kristek & Moczo 2003, Kristek et al. 2002.

2.2.2. ABAQUS

The problem is analysed in the time domain employing the finite element (FE) method. Very finely discretized quadrilateral continuum elements have been used to ensure realistic representation of the propagating wavelengths. Radiation damping is taken into account by introducing appropriate absorbing boundaries at the base of the numerical model. A hybrid “free-field boundary” has been used at the two side boundaries of the model placed at a distance of 1000 m from the valley edge. The latter consists of a 1D soil column (allocated the rock properties) connected with the lateral border nodes of the valley model through Vs and Vp dashpots. Rayleigh damping is introduced to effectively reproduce viscoelastic response, while nonlinear hysteretic soil behaviour is modelled by employing a kinematic hardening constitutive model, incorporating the Von Mises failure criterion and an associative plastic flow rule. The model has been validated against centrifuge experiments, and shown to effectively capture the undrained cyclic soil response [Anastasopoulos et. al., 2011]. The evolution law of the model consists of two components: a nonlinear kinematic hardening component, which describes the translation of the yield surface in the stress space (defined through the "backstress" parameter α), and an isotropic hardening component, which defines the size of the yield surface σ_o as a function of plastic deformation. The model has been successfully adopted in the analysis of the seismic behavior of an alluvial basin by Gelagoti et al. [2010].

2.2.3. FLAC2D

FLAC2D uses the explicit FD method, solving the full equations of motion in the time domain. The discretisation was performed so as to allow frequencies up to 10 Hz to propagate without distortion through the grid. Maximum allowed zone size is 10 times smaller than the minimum wavelength. The two sides of the model were considered as free-field boundaries (Cundall et al., 1980). The base was considered a viscous boundary, since it does not represent an existing soil interface but a continuation of the same material. Such boundaries are described by Lysmer and Kuhlemeyer (1969) and use independent dashpots in the normal and shear direction to the boundary. The critical time step of the dynamic analysis is calculated internally by the code based on the P-wave velocity, area and dimensions of each zone in the grid. The isotropic linear elastic constitutive model was used. Material damping was introduced into the calculations to account for energy dissipation. Mass- and stiffness-proportional Rayleigh type of inelastic damping was used. The average damping value for each material was centered around a central frequency of 2.4 Hz. This provides relatively frequency-independent damping for the frequency range we are most interested in (i.e., from 1 to 6 Hz), which includes most of the model's natural frequencies as well as the predominant input frequencies. Details could be found in Ktenidou (2010). To implement non-linearity, a 1D equivalent linear analysis was first carried out, so as to estimate the strain-compatible soil properties of the surface soil layer based on the given G-γ-D curve. This means that the discretisation made based on elastic parameters is acceptable and we need not repeat it, and the same holds for the initial static stress calculations.

3. SEISMIC RESPONSE OF THE 2D VALLEY MODEL

We have computed synthetic seismic motion (30sec time histories of ground acceleration, velocity, displacement) at 51 locations/receivers (triangles in figure 1) at the free surface of the 2D model both within and outside the valley configuration. Table 2 shows a summary of cases analyzed per numerical code. To what follows in section 3.1, we have chosen to compare and present synthetic velocity time histories as a compromise between high frequency acceleration and low frequency displacement synthetic motion. In section 3.2, we present aggravation factors defined as the ratio between 2D and 1D acceleration response spectra, for a series of cases (4, 6, 7, 8 and 9 of table 1).

Table 2. Summary of cases analyzed per numerical code

	Case 1	**Case 2**	**Case 4**	**Case 6**	**Case 7**	**Case 8**	**Case 9**
ABAQUS	X	X	X	X	X	X	X
FLAC	X	X	X	X		-	-
FD	X	X	X	-	-	-	-

3.1 Elastic and Viscoelastic cases

The first step of the verification test consists in computing the purely elastic response (case 1) in order to check the implementation and performance of boundary conditions with each numerical method used. A representation of the synthetic seismograms section of FDDVS algorithm is given in figure 3. It is immediately evident that a) the wavefield within the valley is dominated by laterally propagated surface waves generated at its edges, b) the amount of backscattered energy is limited and c) the performance of the lateral sides boundary conditions is fine. The absence of inelastic attenuation in this case, despite the fact that leads to an overestimation of amplitudes, allow us, first, to identify the most important features of the synthetic motion and second, to observe the maximum differences in the computed motion introduced by the numerical methods themselves. Figure 4 shows the comparison between synthetic seismograms for the 3 numerical methods. We have chosen to give their comparison for the closest to the valley "rock" receiver (No 20, fig. 4 – left) and that located at its centre (No 51, fig. 4 – right). We observe that the agreement in the time representation of synthetic ground motion either outside or within the valley is surprisingly good if we think of the different way each numerical method "see" this 2D valley model. It could be claimed that the 3 seismograms at receiver No20 is almost identical, while notable but still small differences are observed at the centre of the valley, especially for that part of the seismogram, which is related with the locally generated

surface waves. The same conclusions are also valid for the rest locations where synthetic motion is computed but not presented.

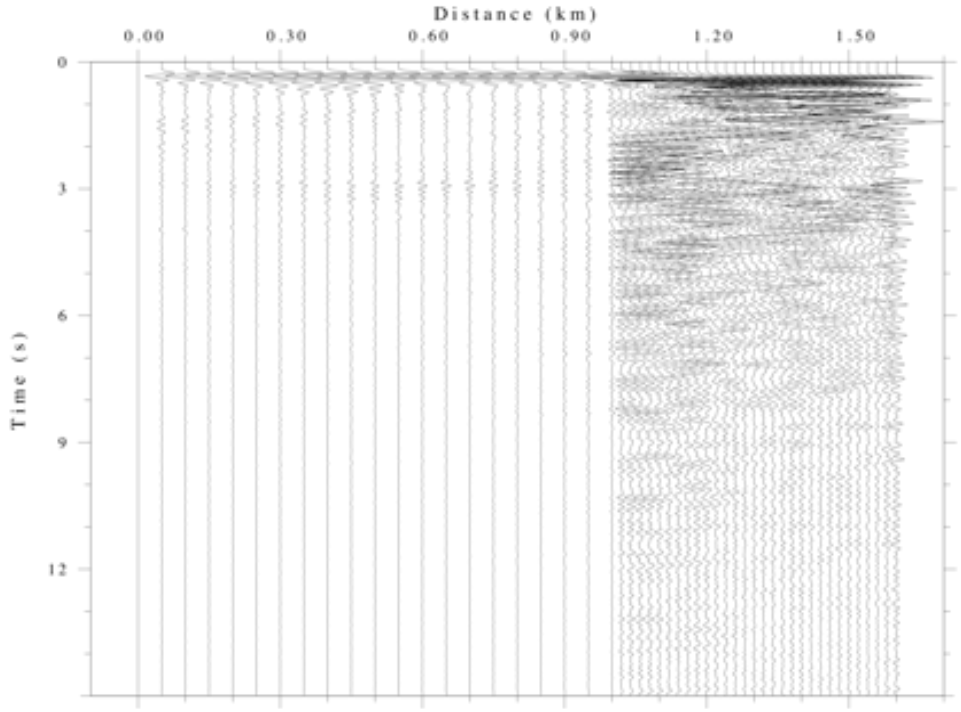

Figure 3. Seismograms sections along the 2D model of figure 1 for CASE 1 and for FDDVS numerical method

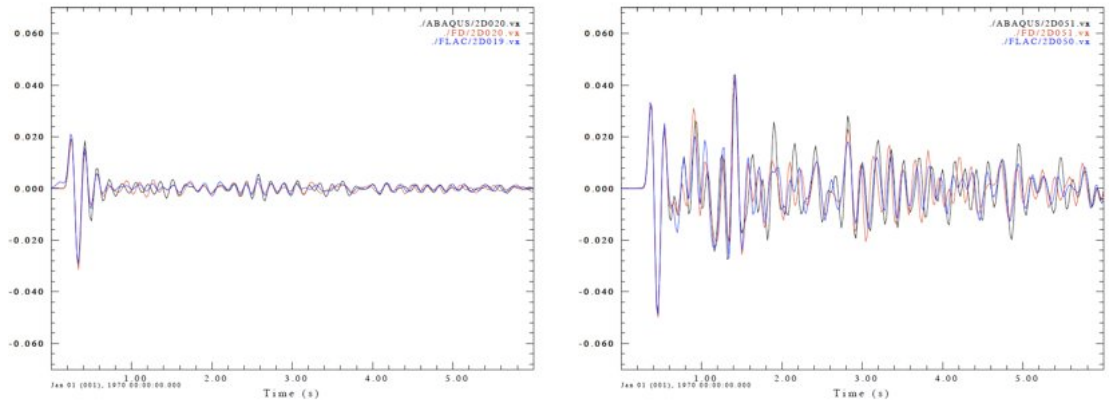

Figure 4. Synthetic seismograms (m/sec) for CASE1 at the receivers No 20 (left) & 51 (right) for ABAQUS (black), FDDVS (red) and FLAC (blue).

The second step of this test was to incorporate inelastic attenuation to our computations (case 2). Given the fact that inelastic attenuation is tackled quite differently between the analysis tools (see section 2.2), one would expect that this will distort the observed agreement for the elastic case at specific frequency ranges. On the contrary, the comparison result between the 3 synthetic seismograms at the centre of the valley is again good (fig. 5 – left). In conjunction with figure 4 (right), we see that inelastic attenuation affected more the amplitude of surface than body waves, a fact related with the distance each type of wave propagates (surface waves travel longer paths than body ones). Figure 5 (right) shows the corresponding frequency representation of synthetic motion with the form of transfer functions (from now on TF). These are computed as the ratio between the synthetic seismogram at the site with the incoming velocity wavefield, and corrected for the free surface effect. It is evident that there is conformity in representing both frequency and amplitude for fundamental and higher resonant modes.

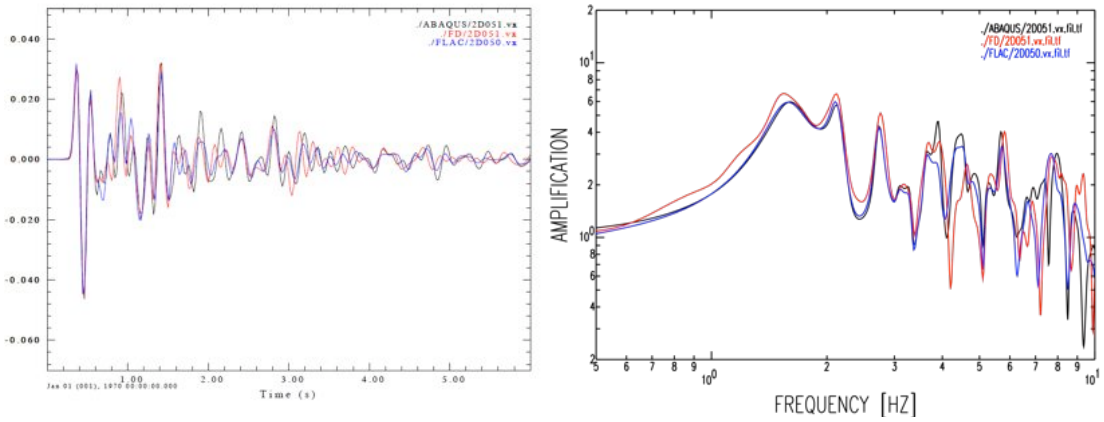

Figure 5. Synthetic seismograms (m/sec) (left) and transfer functions (right) for CASE2 at receiver 51 for ABAQUS (black), FDDVS (red) and FLAC (blue).

Having in mind that the amount of diffracted energy that is trapped within the valley strongly depends on the shear wave velocity contrast between sediments and surrounding rock material, we decided to compute the same valley configuration with Vs contrast equal to 6 (case 4) instead of 4 (case 2), in order to test the efficiency of our numerical tools to this parameter too. Vs values for cases 2 and 4 are given in table 1. Good agreement is observed in both time and frequency domains among results from the 3 analyses (fig. 6). Indeed, amplitude of diffracted surface waves is larger than those of previous case 2 (figure 5, left), as well as amplification of ground motion. Fundamental and higher modes frequencies are now shift to lower values, as the result of reducing Vs for the material filling the valley.

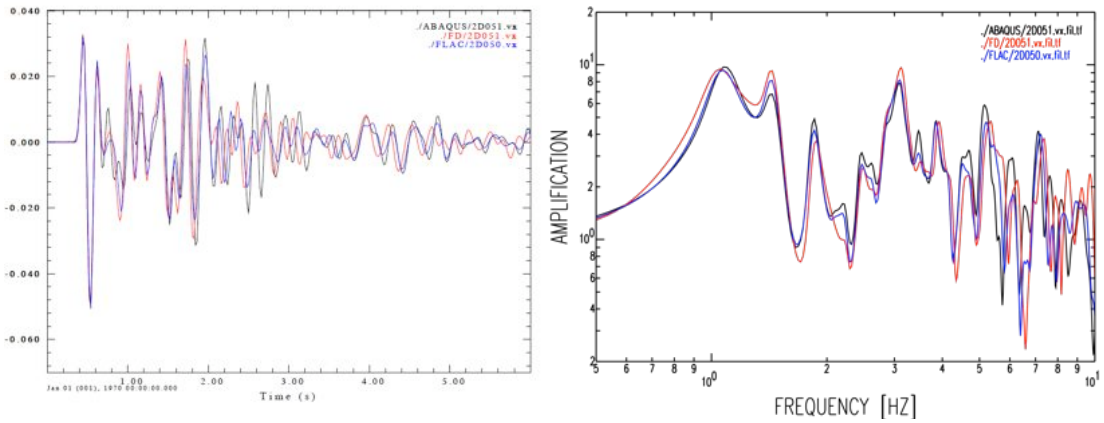

Figure 6. Synthetic seismograms (m/sec) (left) and transfer functions (right) for CASE4 at receiver 51 for ABAQUS (black), FDDVS (red) and FLAC (blue).

3.2 Non-linear cases

Till now, we have presented results that prove the efficiency of the numerical tools used to reproduce complex seismic wavefields in the elastic range with and without inelastic attenuation as well as for different Vs contrasts. Willing to check the coupling of non-linear effects with the geometrical characteristics of the basin, we have computed the response of the same valley (case 4) for a series of input motion levels (0.1g, 0.3g, 0.5g and 1g motion) using either the equivalent linear approximation (FLAC2D) or non-linear behaviour (ABAQUS). These are cases 6 to 9 in table 1 respectively. We only present results obtained by ABAQUS, to give attention to the effects that a “fully” non linear approach will have on the results, given the limitations of the equivalent linear approximation to accurately reproduce dynamic behaviour of soil material for large strain levels. We use case 4 (viscoelastic case) as reference in order to conclude on the effect of nonlinearities on the

characteristics of computed ground motion.

Figure 7 presents a summary of synthetic seismograms (left) and TFs (right) at the centre of the valley for cases 4, 6-9. Note that seismograms (fig. 7 left) are stored with increasing input motion level (top to bottom) and that amplitude scale is not the same. We observe that results for case 4 and 6 are almost identical, meaning that the response of the valley is linear for input motion levels up to 0.1g. Non-linear effects are more pronounced for cases 7-9. There is a clear decrease in the amplification of ground motion (fig. 7 – right) with increasing input as the result of the hysteretic attenuation increase. The amplification decrease is observed to be greater for higher modes mostly related with diffracted wavefields than for the fundamental one. On the other hand, we can see a slight shift of fundamental frequencies towards lower values, that one would expect to be more pronounced with increasing input motion level up to 1g (outcrop). This probably indicates that the calibration of the constitutive model to the G-γ-D (fig. 2) results to hysteresis loops of similar shear modulus but with increasing area, and thus, hysteretic damping.

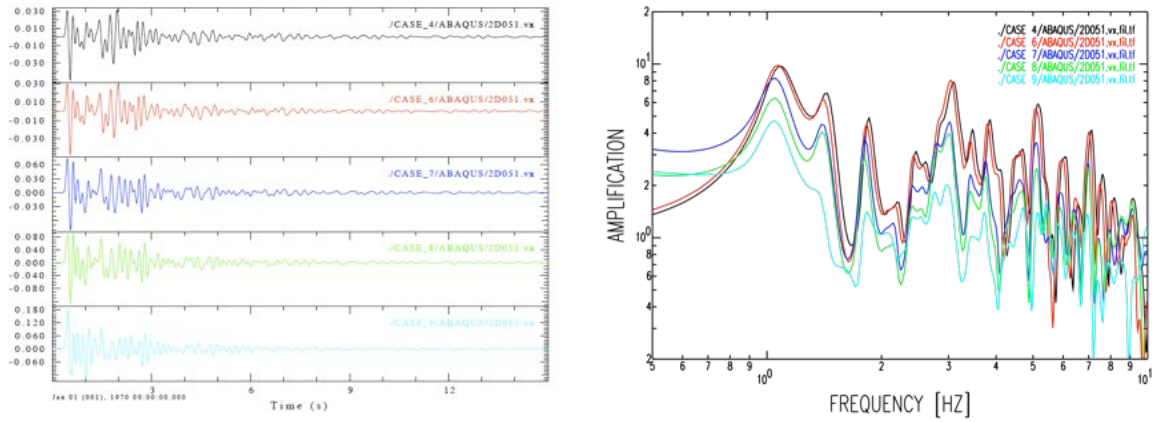

Figure 7. ABAQUS synthetic seismograms (m/sec) (left) and transfer functions (right) for CASE4 (black), CASE6 (red), CASE7 (blue), CASE8 (green) and CASE9 (cyan)

3.3 Aggravation factor

In this section, we take advantage of the results already discussed and present them with the form of aggravation factors. These factors are introduced to quantify the additional amplification in response spectra by the 2D nature of the response at this valley, relative to the amplification that could be predicted using a 1D model. They are defined as the ratio between 2D and 1D acceleration response spectra. To achieve that, we made use of ABAQUS 2D acceleration time histories to compute their response spectra as well as local 1D synthetic acceleration time histories and spectra, for cases 6 to 9. The purpose is to distinguish general trends in their shape (amplification and period changes) in two ways: a) along the 2D model and b) among different excitation levels.

After a careful evaluation of the aggravation factors one by one, we found out that they can be categorized in three groups along the valley configuration of figure 1. Figure 8 shows the proposed categorization along the valley for cases 6, 8 and 9. The first group (fig. 8 – left) refers to the receivers on rock sites outside the valley for which the aggravation factor is, as expected, almost 1 for the whole examined period range (0.1 to 3 sec). The second group stands for the locations inside the sedimentary valley at distances between 0 and 120m (0-1.2 times the maximum depth of the valley) from the edge (fig. 8 – middle). The aggravation factors determined for this group have varying with period amplitudes, generally, smaller than 1. This means that 1D seismic response for these sites is larger than 2D one. This observation could be attributed with the fact that for 1D analyses, the amount of energy which is trapped within the sedimentary layer, leading to resonance, is larger than that for 2D, since part of the energy is diffracted at the lateral sides and generates surface waves. The third group is then formed with the rest sedimentary sites (fig.8 – right). The aggravation factor for this group is

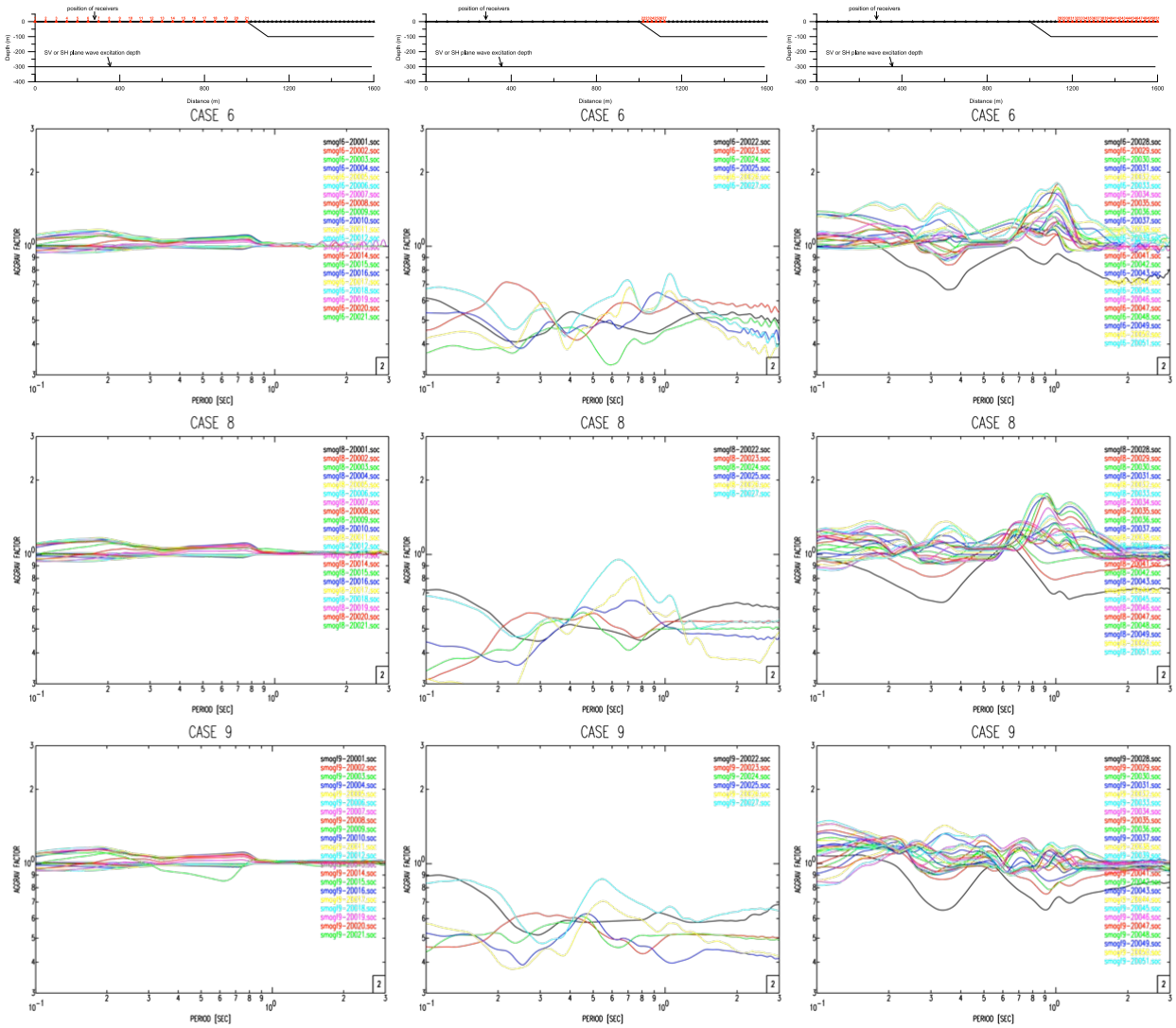

Figure 8. Categorization of aggravation factors along the valley: rock sites (left), close to edge sites (middle) and middle sites (right) for cases 6 (1st row), 8(2nd row) and 9 (3rd row)

generally larger than 1. The maximum value is around 2 for the fundamental period of the sedimentary layer. Nevertheless, for case 9 with the highest excitation level that corresponds to 1g outcrop), the aggravation factor of the third group is per average 1, which means that hysteretic attenuation is so high that wipes out dramatically surface waves. It is worth noticing that even for strong excitation (0.5g outcrop – case 8), the aggravation factor within the valley could be of the order of 1.5 or more.

A more precise representation of the evolution of the aggravation factors within the valley is given in figure 9. We, there, plot together AFs for cases 4, 6-9 for selected locations starting from the edge towards the centre of the valley. Receivers 22, 24, and 26 belong to the second group according to our previous comments, while the rest receivers to the third one. It is clear that amplitude of aggravation factor is gradually increased while moving to the centre of the valley and that from receiver 35 to 51, the increase in the amplitude is observed at the fundamental frequency of the sedimentary layer.

4. CONCLUSIONS

We have presented results of 3 different numerical tools (FDDVS, FLAC and ABAQUS) and checked their efficiency in reproducing complex (2D) seismic wavefields up to 10Hz for a specific two-dimensional trapezoidal basin. A basic element of this work was to incorporate the non-linear dynamic

behaviour of soil and to check the coupling of non-linear effects with the geometrical characteristics of the basin for a series of excitation levels (0.1g, 0.3g, 0.5g and 1g outcrop). Extensive comparisons are made both in time (synthetic velocity time histories) and frequency (amplification transfer functions) domain, as well as in terms of aggravation factors at specific locations along the surface of the 2D basin.

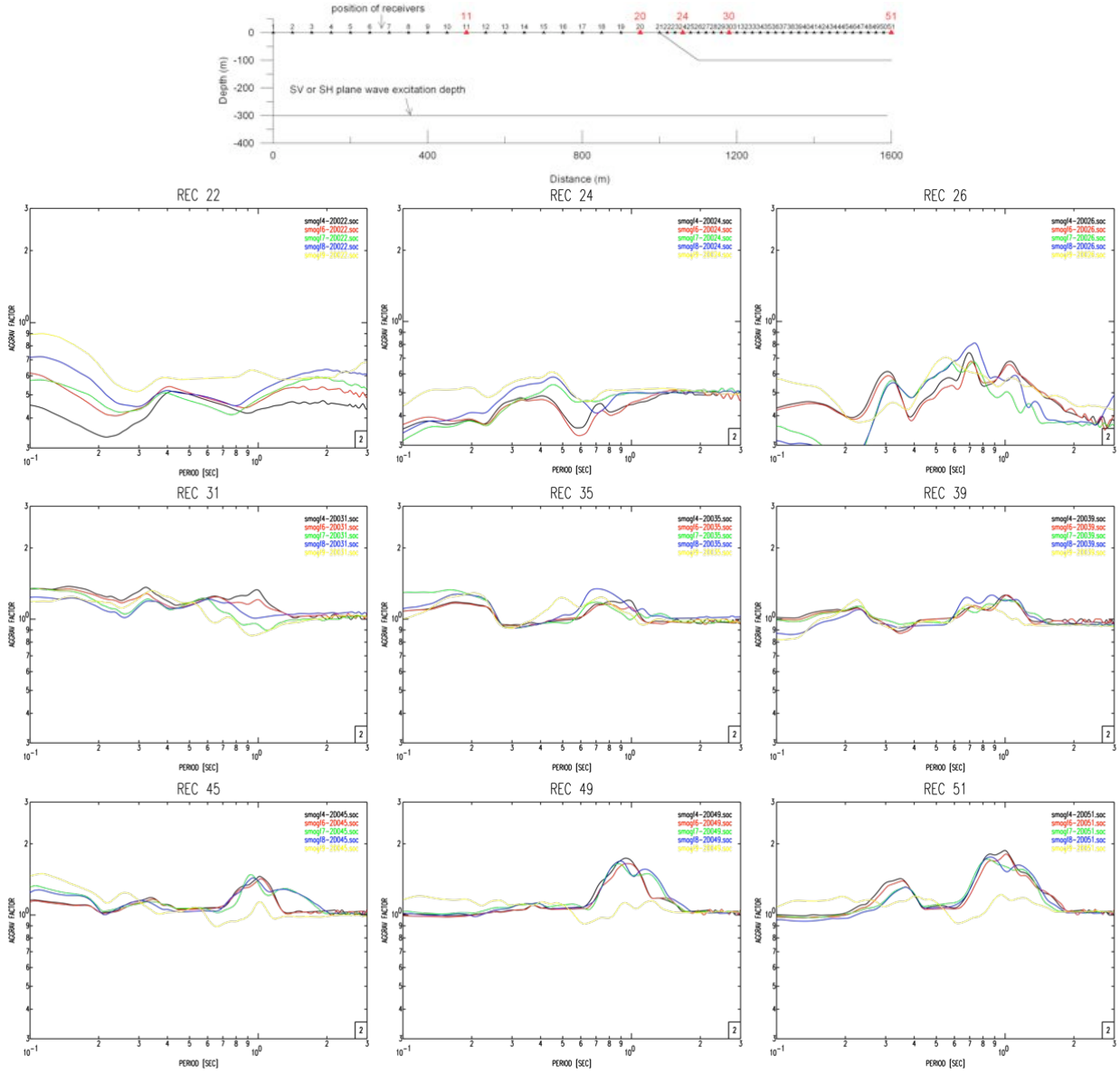

Figure 9. Comparison of aggravation factors for CASES 4, 6, 7, 8, 9 at specific positions along the sedimentary valley

The agreement in the results of the 3 numerical tools is surprisingly good given the different approaches (FD vs FE, boundary conditions, attenuation, constitutive law) implemented in each one. All of them are in the position to "accurately" reproduce the complexity in the characteristics of seismic motion for this model configuration. This suggests that each code in itself or in combination can be safely used to perform the necessary parametric analyses. We have also shown that it is possible to consolidate practical guidelines in order to introduce basin effects in the seismic design of structures. Aggravation factors could be one of these guidelines that depend more on the position along the valley than on excitation motion level.

AKCNOWLEDGEMENT
The work presented in this paper is funded by the European Community's Seventh Framework Programme [FP7/2007-2013] under grant agreement n° 262330 entitled NERA: Network of European Research Infrastructures for Earthquake Risk Assessment and Mitigation.

REFERENCES

ABAQUS, Inc. (2008), *ABAQUS user's manual*, Providence, R.I.

Aki, K. (1993). Local site effects on weak and strong ground motion. *Tectonophysics*, 218,93-111.

Anastasopoulos I., F. Gelagoti, R. Kourkoulis & G. Gazetas. 2011. Simplified Constitutive Model for Simulation of Cyclic Response of Shallow Foundations : Validation against Laboratory Tests. J. Geotech. Geoenv.. Engng ASCE **137: 12**, 1154–1168.

Bard, P.-Y. (1994). Effects of surface geology on ground motion: recent results and remaining issues. *Proc. 10th European Conf. Earthq. Eng.*, **1**:305-323.

Chávez-García, F.J., L.R.Sanchez and D. Hatzfeld (1996). Topographic site effects and HVSR. A comparison between observations and theory. *Bull. Seism. Soc. Am.,* **89:3**, 1559-1573.

Chávez-García, F.J., D. Raptakis, K. Makra & K. Pitilakis, 2000. Site effects at Euroseistest II. Results from 2D numerical modelling and comparison with observations. *Soil Dyn. Earthq. Eng.,* **19:1**, 23-39.

Cundall, P. A., H. Hansteen, S. Lacasse and P. B. Selnes (1980). NESSI — Soil Structure Interaction Program for Dynamic and Static Problems, Norwegian Geotechnical Institute, Report 51508-9.

Faccioli, E., 1991. Seismic amplification in the presence of geological and topographic irregularities. *Proc. 2nd Intern. Conf. On Recent Advances in Geotechnical Earthq. Engrg.*, State-of-art paper, 1779-1797.

Gelagoti F., R. Kourkoulis, I. Anastasopoulos, T. Tazoh, and G. Gazetas, (2010), "Seismic Wave Propagation in a Very Soft Alluvial Valley: Sensitivity to Ground-Motion Details and Soil Nonlinearity, and Generation of a Parasitic Vertical Component", *BSSA*, Vol. **100(6)**, pp. 3035-3054

ITASCA (2005). FLAC – Fast Lagrangian Analysis of Continua – Version 5.0. User's Guide, Itasca Consulting Group, Minneapolis, USA.

Kawase, H., 1996. The cause of damage belt in Kobe: "The basin edge effect", Constructive interference of the direct S-wave with the basin induced diffracted/Rayleigh waves. *Seism. Res. Letters*, **67:5**,25-34.

Kristek, J. and Moczo, P. (2003). Seismic wave propagation in viscoelastic media with material discontinuities – a 3D 4th-order staggered-grid finite-difference modeling. *Bull. Seism. Soc. Am.* **93**,2273-2280.

Kristek, J., Moczo, P. and Archuleta, R.J. (2002). Efficient methods to simulate planar free surface in the 3D 4th-order staggered-grid finite-difference schemes. *Studia Geophys. Geod.* **46**,355-381.

Ktenidou, O.-J. (2010). Theoretical and instrumental study of site and topographic effects on strong ground motion in Aegion, Ph.D. Thesis, Aristotle University, Thessaloniki, Greece. Available in electronic format at: http://invenio.lib.auth.gr/record/124050/files/GRI-2010-5489.pdf.

Lysmer, J., and R. L. Kuhlemeyer (1969). Finite Dynamic Model for Infinite Media, J. Eng. Mech., 95, pp. 859-877.

Makra, K., D. Raptakis, F.J. Chávez-García & K. Pitilakis (2001). Site effects and design provisions: The case of EUROSEISTEST. *Pure and Applied Geophysics*, **158:12**,2349-2367.

Makra K., F.J. Chávez-García, D. Raptakis & K. Pitilakis (2005). Parametric analysis of the seismic response of a 2D sedimentary valley: Implications for code implementations of complex site effects. *Soil Dynamics & Earthquake Engineering,* **25**, 303-315.

Makra, K. & D. Raptakis (2007). How Sensitive The Effects Of Lateral Heterogeneity On Seismic Ground Motion Are? *Proc. of the 4th International Conference on Earthquake Geotechnical Engineering*, CDROM Paper No. 1687.

Moczo, P., Kristek, J., Galis, M., Pazak, P. and Balazovjech, M. (2007). The Finite Difference and Finite-Element Modeling of Seismic Wave Propagation and Earthquake Motion. *Acta Physica Slovaca* **57**,177-406.

Moczo, P., Kristek, J. and Galis, M. (2004). Simulation of planar free surface with near-surface lateral discontinuities in the finite-difference modeling of seismic motion. *Bull. Seism. Soc. Am.* **94**,760-768.

Pitilakis, K, D. Raptakis, K. Makra, M. Manakou and F.J. Chávez-García (2011). Euroseistest 3D Array for the Study of Complex Site Effects, *Geotechnical, Geological and Earthquake Engineering*, **14:3**, 145-166, DOI: 10.1007/978-94-007-0152-6_11

Pitilakis, K., D. Raptakis, K. Lontzetidis, Th. Tika-Vassilikou & D. Jongmans (1999). Geotechnical & geophysical description of EURO-SEISTEST, using field, laboratory tests and moderate strong motion recordings. *J. of Earthq. Eng.*, **3:3**,381-409.

Raptakis, D., F.J. Chávez-García, K. Makra & K. Pitilakis, 2000. Site effects at Euroseistest I: Determination of the valley structure and confrontation of observations with 1D analysis. *Soil Dyn. Earthq. Eng.,* **19:1**,1-22